EEET ECOLOGICAL ENGINEERING & ENVIRONMENTAL TECHNOLOGY

Ecological Engineering & Environmental Technology, 2025, 26(1), 305–315
https://doi.org/10.12912/27197050/196040
ISSN 2719–7050, License CC-BY 4.0

Received: 2024.11.01
Accepted: 2024.11.27
Published: 2024.12.01

Modification of activated carbon from processed salak fruit waste with Fe_3O_4 composite for removal of Pb(II) in wastewater

Esthi Kusdarini[1*], Maritha Nilam Kusuma[2], Agus Budianto[1], Eva Atiyatussa'adah[1], Edo Augusta Garino[1]

[1] Faculty of Industrial Technology, Adhi Tama Institute of Technology Surabaya, Jl. Arief Rachman Hakim 100, Surabaya, Indonesia
[2] Faculty of Civil Engineering and Planning, Adhi Tama Institute of Technology Surabaya, Jl. Arief Rachman Hakim 100, Surabaya, Indonesia
* Corresponding author's e-mail: esti@itats.ac.id

ABSTRACT

Pb(II) is a heavy metal that is harmful to health and the environment. This metal is often found in industrial waste so it needs to be removed. One way to reduce these heavy metals is to use activated carbon. Various types of organic materials and agricultural waste can be made into activated carbon.. One of the agricultural wastes that has great potential as activated carbon is salak seeds. This research processed salak seeds into activated carbon and modified them into Magnetic Activated Carbon (MAC). The research aims to obtain: 1) the best operating conditions for activated carbon production and MAC; 2) characteristics of activated carbon and MAC; 3) % removal of Pb(II) from liquid waste with MAC; 4) isotherm adsorption equation Pb(II) by MAC; 5) the kinetics equation of Pb(II) adsorption by MAC. The research method is to make activated carbon by carbonization, chemical and physical activation. The chemical activator used is a mixture of phosphoric acid – hydrochloric acid with a composition (1: 1). The next step is to make a MAC from activated carbon. Activated carbon characteristics were tested using the BET, SEM, EDX, and ASTM standard proximate tests. The results showed that activated carbon met SNI standards with iodine number 1230.93–1256.31 mg/g, surface area 539.147 m2/g, pore volume 44.0262–112.5906 cc/g. MAC contains 1% water, 21.88% volatile matter, 38% ash, 39.12% fixed carbon, and 1243.62 mg/g iodine number. Further findings show that the adsorption isotherm equation is best using the Freundlich equation. The Freundlich equation constants n = 1.3530 and K_F = 34.634 mg/g with R^2 = 0.913, while the Langmuir equations b = 0.7442 L/mg and qm = 78.125 mg/g with R^2 = 0.6692. The Pb(II) adsorption kinetics test by MAC showed pseudo-2nd order adsorption kinetics with the constant k_2 = 0.2737 g/mg.min and R^2 = 1.

Keywords: carbon active magnetic, friendly, Langmuir, Pb(II), salak seeds.

INTRODUCTION

Currently, industries around the world are growing rapidly. This is very helpful in improving human welfare. However, this also has a negative impact with waste produced by the industry. One of the wastes produced by the chemical industry that is harmful to health is lead. Lead in wastewater in the form of Pb(II) ions when accumulated in the human body can cause various health disorders that attack several organs and nerves. This condition has caused several studies to be conducted to eliminate the Pb(II) ion content in industrial waste. (Ahmad and Manefield, 2024; Cai et al., 2025; Chaurasia and Kumar, 2024; Ismail et al., 2024; Mohamed et al., 2024; Pochampally et al., 2024; Yokwana et al., 2024).

Meanwhile, to support clean production, several studies use agricultural waste to remove Pb(II) ions (Ahmad and Manefield, 2024; Ahmed et al., 2024; Ali et al., 2024; Gargiulo et al., 2024; Messaoudi et al., 2024; Pochampally et al., 2024; Ton-That et al., 2024; Yokwana et al., 2024). Research by Ahmed et al. (2024) reviewed Pb(II) adsorption technology using activated carbon made from agricultural waste, which showed an

increase in the efficiency of removing Pb(II) from wastewater (Ahmed et al., 2024). In addition, research by Ali et al. (2024) examined the potential of sunflower waste to reduce Pb(II), showing promising results in reducing the toxicity of Pb(II). The adsorption method with activated carbon is effective in reducing heavy metals. This happens because activated carbon is a common adsorbent. Adoption is easy and economical in its application.

Some organic materials containing carbon, such as agricultural waste, have the potential to be made into activated carbon. Snake fruit seeds (*Salacca zalacca*) are waste from the snake fruit processing industry that are widely found in the city of Yogyakarta, Indonesia. Snake fruit seeds have the potential to be made into activated carbon, but can only be used once in processing. This study will modify the method of making activated carbon from snake fruit seeds by adding Fe_3O_4 composite to become MAC. Modification of activated carbon into MAC is expected to save processing costs for heavy metal removal because it can be used repeatedly. Macs can be separated from industrial waste with the help of magnets.

The manufacture of activated carbon from snake fruit seeds has two functions. The first function is to process agricultural waste and the second function is to obtain an adsorber to process industrial waste. The process of making activated carbon is generally through activation, either through soaking using chemicals or heating at a certain temperature. Modification of activated carbon into MAC makes it reusable after being contacted with wastewater. Several studies have shown that MAC is more efficient at removing heavy metals from industrial waste than conventional activated carbon (Alam et al., 2024; Altintig et al., 2018; Bagbi et al., 2024; Gong et al., 2017; Liu et al., 2019; Samanth et al., 2024; Vaddi and Malla, 2024; Wei et al., 2023; Yang et al., 2023). Various studies on the manufacture of MAC have been carried out but those made from activated carbon derived from salak seeds are not yet available. Research on making MAC from activated carbon derived from Salak seeds is very interesting to do.

This research aims to develop an efficient KAM manufacturing method for the production of MAC from salak seeds through the process of physical-chemical activation followed by the activation of a magnetic solution, Fe_3O_4 composite. The second objective is to characterize the resulting MAC using BET to know surface area and pore volume and SEM EDX to view morphology and proximate tests. The third objective was to test the performance of MAC in removing lead ions from wastewater solutions through batch reactor, parameter is the concentration of lead in wastewater. The fourth objective is to model the kinetics and isotherms of adsorption to understand the mechanism of interaction between MAC and Pb(II) ions.

MATERIALS AND METHODS

Materials

Experiments require materials were salak seeds, $Pb(NO_3)_2$, $FeSO_4.6H_2O$, NH_4OH 25% Pro Analyst, $FeCl_3.6H_2O$, H_3PO_4 Pro Analyst 85%, KOH, HCl 37%, amylum, iodine, $Na_2S_2O_3.5H_2O$ Pro Analyst, H_2CrO_4, and aquadest. Meanwhile, the tools used are hammers, grinders, analytical balances, droppers, measuring flasks, clamps, filter paper, burettes, furnaces, beaker glass, aluminium foil, funnels, measuring cups, and Erlenmeyer.

Methods

Magnetic-activated carbon manufacturing

The steps to make activated carbon are: 1) washing salak seeds; 2) dry the salak seeds for 1 hour; 3) carbonization, which is heating salak seeds at a temperature of 350 °C for 5 hours; 4) sieving with a sieve of 60 mesh; 5) separating salak seed granules < size 60 mesh to be used as activated carbon raw materials; 6) chemical activation, namely soaking salak charcoal in a combined chemical activator HCl and H_3PO_4 (CCAHH) for 24 hours with a ratio of molarity (1 : 1) and volume (1 : 1) variable dose 0.55 M (sample A); 1.05 M (sample B); 1.55 M (sample C); 2.05 M (sample D); and 2.55 M (sample E); 7) neutralize salak seed charcoal using 0.1 M NaOH, aquadest, using filter paper to separate activated charcoal from the solution; 8) storing chemically activated activated carbon in aluminum foil for iodine number analysis; 9) store chemically activated activated carbon with the best iodine number for analysis with EDX BET and SEM equipment; 10) physical activation, namely heating the activated carbon of salak seeds at a temperature of 600 °C (samples A1, B1, C1, D1); 10) storing samples A1, B1, C1, D1 for analysis of proximate and iodine

numbers; 11) physical chemical activated carbon samples with the best iodine numbers analyzed by BET and SEM EDX; 11) make a magnetic/composite solution of Fe_3O_4 by mixing a solution of $FeCl_3.6H_2O$ and $FeSO_4.6H_2O$ with a ratio of molarity of 1 : 2 and volume of 1 : 1; 12) add the NH_4OH solution drop by drop until the pH reaches 10 while constantly stirring; 13) Physical chemical activated carbon sample with the best iodine number soaked in a magnetic solution of chili sauce stirred with for 30 minutes; 14) neutralize the MAC of salak seeds using aquadest, separating the MAC from the neutralizing solution with filter paper; 14) Heat MAC salak seeds at 100 °C for 4 hours; 11) store the MAC in aluminum foil for analysis of the proximate and iodine number.

Activated carbon characteristic test

The analysis carried out on the sample included 4 types, namely 1) proximate analysis; 2) iodine number analysis; 3) BET analysis, and 4) SEM EDX analysis. Proximate analysis includes:1) water content testing (*wc*); 2) volatile matter content (*vmc*); 3) ash content (*ac*). Next, fixed carbon (fcc) is obtained using Equation 1.

$$wc + vmc + ac + fcc = 100\% \quad (1)$$

Iodine number analysis uses the ASTM D-4607-94 method. Analyze the surface area and pore volume using the BET method. Meanwhile, the surface morphological analysis uses the SEM-EDX method.

MAC adsorption ability test against Pb(II) ions

Testing of MAC adsorption ability against Pb(II) ions contained in $Pb(NO_3)_2$ solution. MAC as much as 1 g was put into 1 L of $Pb(NO_3)_2$ solution 36.44 mg/L (PbI_1 sample); 30.37 mg/L (PbI_2 sample); 24.29 mg/L (PbI_3 sample); 18.22 mg/L (PbI_4 sample); and 12.15 mg/L (PbI_5 sample) were shaken for 3 hours and left for 24 hours. After 24 hours, the solution containing the lead and MAC is separated using filter paper. Furthermore, the lead content in the $Pb(NO_3)_2$ solution was analyzed before contact with activated carbon (initial Pb) and after contact with MAC (final Pb) using the AAS method (SNI 6989.71:2009). The percentage of Pb(II) ions absorbed by MAC was obtained using Equation 2.

$$\%\ removal\ lead\ (Pb) = \frac{Pb\ in - Pb\ out}{Pb\ in} \times 100\% \quad (2)$$

Furthermore, the adsorption ability of MAC to Pb(II) ions was also carried out with a variable MAC contact time with $Pb(NO_3)_2$ solution. The sampling was carried out by making 10 sample solutions. Ten pieces of $Pb(NO_3)$ solution volume 1 L concentration of 36.44 mg/L which each has been added 1 g of MAC to it, then shaken, and each solution is taken one after another with variable time: Pbk_1 (1 min), Pbk_2 (3 min), Pbk_3 (5 min), Pbk_4 (10 min), Pbk_5 (30 min), Pbk_6 (60 min), Pbk_7 (75 min), to then be separated by MAC using filter paper and chromium content analysis using the AAS method (SNI 6989.71:2009) on 7 solutions that have been separated from MAC.

Adsorption isotherm equation test

The isotherm equation test aims to determine the amount of Pb(II) ions that can be adsorbed by magnetic activated carbon from salak seeds. The equations tested are Freundlich and Langmuir. The Freundlich equation is presented in Equation 3.

$$log\ q_e = log\ K_F + \frac{1}{n}\ log\ C_e \quad (3)$$

where: q_e is ion equilibrium capacity that is number of ions Pb(II) adsorbed per unit mass of MAC (mg/L), C_e is the concentration of Pb(II) ions in waste water at equilibrium conditions after the adsorption process by MAC (mg/L). The next step is to make a graph of log C_e versus log q_e to get Equation 3 so that the K_F and n values are obtained.

The second isotherm adsorption equation tested was the Langmuir equation, which is presented in Equation 4.

$$\frac{C_e}{q_e} = \frac{C_e}{q_m} + \frac{1}{bq_m} \quad (4)$$

In this equation q_e (mg/g) is the mass of Pb(II) ions adsorbed by each unit mass of MAC. c_e (mg/L) is the concentration of Pb(II) ions in waste water under equilibrium conditions. While b (L/mg) and q_m (mg/g) are the constants. The values of b and q_m are obtained by plotting a graph of c_e versus $\frac{C_e}{q_e}$.

Adsorption kinetics model test

The analysis of the adsorption kinetic model was obtained by testing the reaction order from 0 to pseudo order 2 (Kusdarini et al., 2023). Linear reactions of the zero-order are expressed by Equation 5.

$$C_t = C_o - k_0 \cdot t \quad (5)$$

where: C_t (mg/L) is the concentration of the substance at t, C_o (mg/L) is the concentration of the initial substance (mg/L), t is the time, k_0 (mg/L.minute) is the zero-order reaction rate constant, t is the adsorption contact time (minute). The zero-order reaction equation is obtained through plot t as the x-axis and the value C_t as the y-axis, with slope = k_0 and intercept = C_o. Furthermore, the first-order reaction equation is expressed by Equation 6.

$$ln\ C_t = ln\ C_o - k_1 \cdot t \quad (6)$$

where: C_t is the concentration of the substance at t (mg/L), C_o is the concentration of the initial substance (mg/L), t is the time, k_1 is the first-order reaction rate constant (1/minute), t is the adsorption contact time (minute). The first-order reaction equation is obtained through plot t as the x-axis and the value of ln C_o/C_t as the y-axis, with slope = k_1. Furthermore, the second-order reaction equation is expressed by Equation 7.

$$\frac{1}{Ct} + \frac{1}{Co} = k_2 \cdot t \quad (7)$$

where: C_t is the concentration of the substance at t (mg/L), C_o is the concentration of the initial substance (mg/L), t is the time, k_2 is the second-order reaction rate constant, and t is the adsorption contact time (minute). The second-order reaction equation is obtained through plot t as the x-axis and the value $\frac{1}{Ct}$ as the y-axis, with slope = k_2 and intercept = - $\frac{1}{Co}$. Furthermore, the pseudo-first-order equation is expressed by Equation 8.

$$log\ (q_e - q_t) = log\ q_e - \frac{k_1}{2.303} \cdot t \quad (8)$$

where: q_e is the capacity for Pb(II) ion equilibrium, namely the weight of Pb(II) ions adsorbed per unit mass of MAC (mg/g), *it* is the capacity for the metal ion at time t, the weight of Pb(II) ions adsorbed per unit mass of MAC (mg/g), k_1 is the adsorption rate constant of the pseudo-first-order (1/minute), t is the adsorption contact time (minute). The pseudo-first-order reaction equation is obtained through plot t as the x-axis and the value log ($q_e - q_t$) as the y-axis, with slope = $\frac{k_1}{2.303}$ and intercept = log q_e. Furthermore, the pseudo-second-order equation is expressed by Equation 9.

$$\frac{t}{q_t} = \frac{1}{k_2 \cdot q_e^2} + \frac{1}{q_e} \cdot t \quad (9)$$

where: q_e is the capacity for Pb(II) ion equilibrium, the weight of Pb(II) ions adsorbed per unit mass MAC (mg/g), q_t is the capacity for the metal ion at time t, namely the mass of Pb(II) ions adsorbed per unit mass of MAC (mg/g), k_2 is the constant adsorption rate of pseudo-second-order (g/mg.minute), t is the adsorption contact time (minute). The pseudo-second reaction equation is obtained through plot t as the x-axis and $\frac{t}{q_t}$ as the y-axis, with slope = $\frac{1}{q_e}$ and intercept = $\frac{1}{k_2 \cdot q_e^2}$.

RESULTS

Characteristics of activated carbon with proximate analysis

This study produced the findings of moisture content, volatile matter content, ash content, fixed carbon, and iodine number from Activated Carbon from Salak Seeds (ACSS) after chemical and physical activation. These are presented in Figure 1, Figure 2, Figure 3, Figure 4, and Figure 5.

Figure 1 is the relationship between CCAHH concentration, to the moisture content in the physically activated ACSS at 600 °C. The research provided significant findings. The water content observed in the range of 1–5% is much lower than the maximum standard set by the Indonesian National Standard (SNI) Number 06-3730-1995, which is 15%. These findings are

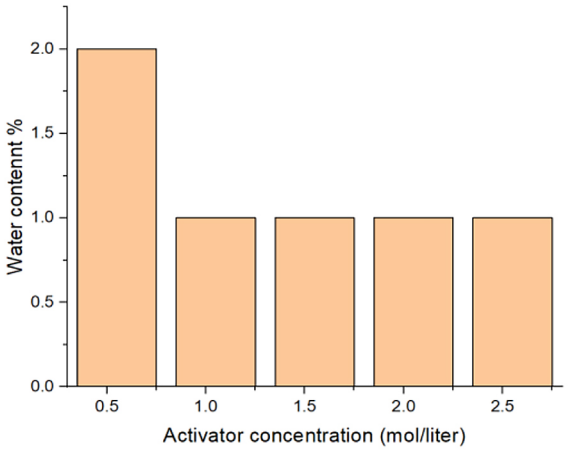

Figure 1. The relationship between CCAHH concentrations at various concentrations on ACSS moisture content and physical activation at 600 °C

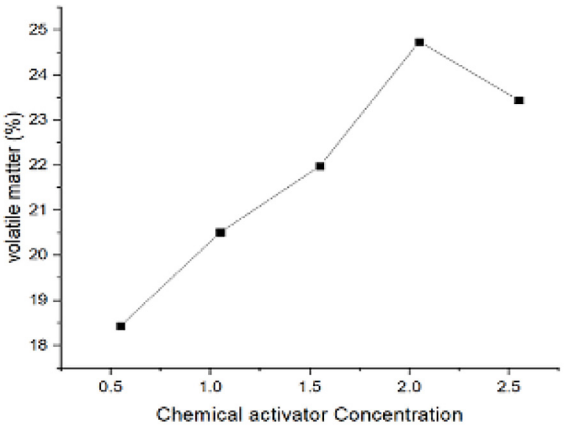

Figure 2. The relationship between CCAHH concentrations at various concentrations of volatile matter from ACSS and physical activation at 600 °C

important because the low moisture content directly contributes to the improvement of ACSS quality, especially in terms of absorbency and stability. Activated carbon with low moisture content usually has a better ability to adsorb gas or liquid molecules because a larger pore area is available for adsorption. The physical activation process, which relies on high temperatures, causes the evaporation of water vapor absorbed in the carbon pores, resulting in carbon with a low moisture content.

Research shows that CCAHH has a crucial role in the ACSS activation process. CCAHH can enlarge pores in the carbon structure, remove volatile substances, and significantly lower moisture content. Previous research has also shown that the higher the activation temperature, the lower the moisture content produced. However, it is important to note that too high an activation temperature can damage the structure of carbon pores and decrease their adsorption capacity. In this case, a temperature of 600 °C is considered optimal because it allows maximum evaporation of water without damaging the resulting pore structure (Alam et al., 2024; Polii, 2017; Vaddi and Malla, 2024; Yue et al., 2003).

ACSS which has a low moisture content as produced in this study has various advantages in industrial applications. The low moisture content not only increases the absorbency but also increases the life of activated carbon because fewer substances need to be adsorbed or absorbed. For example, in water filtration applications, activated carbon with a low moisture content can capture more contaminants and work more efficiently at filtering out small particles, including heavy metals and organic compounds. Activated carbon with low moisture content is also highly desirable in air purification applications because it is more efficient in absorbing harmful gases such as ammonia and sulfur dioxide.

Figure 2 shows the effect of CCAHH concentration on various concentrations of volatile matter content (*vmc*) from ACSS with physical activation at 600 °C. The effect of CCAHH on volatile matter (*vmc*) from ACSS produced from salak seeds with physical activation at 600 °C shows a significant relationship. Based on the research, the volatile matter level produced ranged from 18.44–24.74%, which met the SNI standard for ACSS. An increase in the concentration of the two activators results in an increase in *vmc* in ACSS, which is caused by the absorption of volatile acidic components into the carbon structure during the activation process.

Overall, these findings suggest that activated carbon from salak seeds activated with CCAHH at high temperatures shows an increase in VM that is consistent with the results of previous studies on different materials. The use of CCAHH has proven to be effective in producing ACSS with quality that meets SNI standards and has physical and chemical characteristics that are suitable for industrial applications that require high adsorption capabilities. The results of this study are under the results of other studies from different materials (Beksissa et al., 2021; Budianto et al., 2021; Budianto et al., 2023; Kusdarini et al., 2022; Yagub, Sen et al., 2014).

Figure 3 shows the effect of CCAHH concentrations on various concentrations of ash

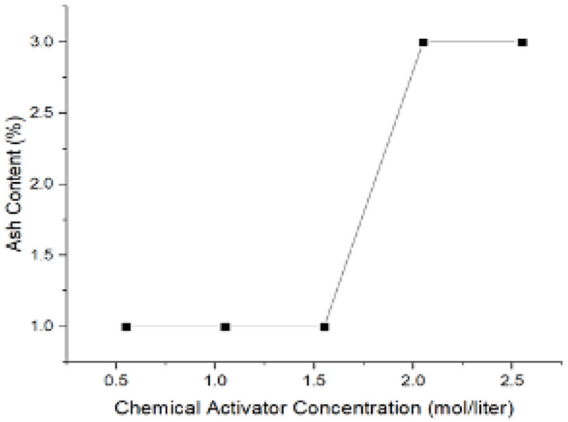

Figure 3. Relationship between CCAHH concentrations at various concentrations on ash content from ACSS and physical activation at 600 °C

content (AsC) from ACSS with physical activation at 600 °C. The results show that AsC ranges from 1–3%. This result shows that ACSS has met SNI standards. The SNI standard requires that the maximum ash content is 10 %. The results of this study have the same trend as the results of previous studies (Beksissa et al., 2021; Agus Budianto et al., 2021, 2023; Kusdarini et al., 2022; Yagub et al., 2014).

Figure 4 shows the effect of ACAHH concentrations on various concentrations of fixed carbon (FC) from ACSS with physical activation at 600 °C. The results show that FC ranges from 68.56–78.56%. These results show that the activated carbon from salak seeds has met SNI standards. The SNI standard requires that the FC is at least 65%. An increase in CCAHH concentration indicates a decrease in FC from ACSS. This happens because of the absorption of chemical activators in ACSS which is a type of volatile acid, so it is part of the VM so that it lowers FC. The results of this study are under the results of previous peeling (Beksissa et al., 2021; Agus Budianto et al., 2021, 2023; Kusdarini et al., 2022; Yagub et al., 2014).

Figure 5 shows the effect of CCAHH concentrations at various concentrations on the absorption of iodine (IN) from ACSS with physical activation at 600 °C. The results show that the IN ranges from 1205.6–1243.6 mg/g. These results show that the activated carbon from salak seeds has met SNI standards. The SNI standard requires that the minimum iodine number is 750 mg/g. The increase in CCAHH levels indicates an increase in IN from ACSS to reach a chemical activator concentration of 2.0 M and then decrease. This occurs due to an increase in fixed carbon levels and an increase in pore volume from activated carbon after activation (Beksissa et al., 2021; Agus Budianto et al., 2021, 2023; Kusdarini et al., 2022; Yagub et al., 2014).

Activated carbon from salak seeds that have been chemically activated by physics and made by MAC has been tested for parameters of moisture content, ash content, volatile matter, fixed carbon, and iodine number as presented in Table 1.

MAC characteristics

Table 1 shows the results of the MAC characteristics test, this table shows that MAC has a better iodine number than the iodine number of conventional activated carbon.

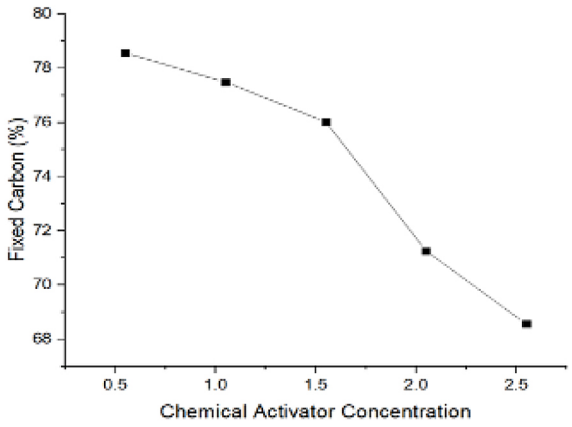

Figure 4. Relationship between CCAHH concentrations at various concentrations of carbon fixe from ACSS and physical activation at 600 °C

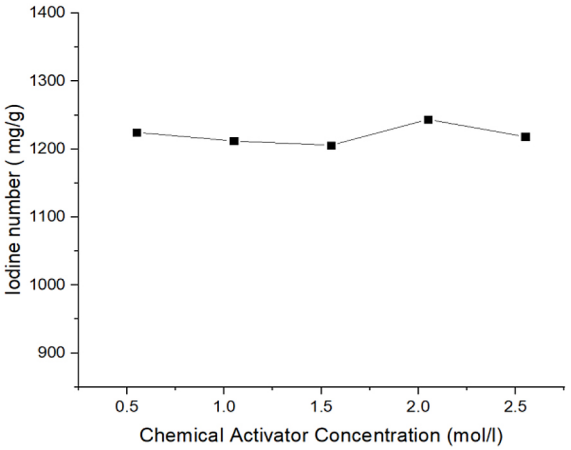

Figure 5. Relationship between CCAHH concentrations at various concentrations on the aerosol power of ACSS and physical activation at 600 °C

Table 1. MAC characteristics

Parameter	Value
Water Content	1.00%
Ash Content	21.88%
Volatile matter	38.00%
Fixed carbon	39.12%
Iodin number	1243.62 mg/g

Analysis of surface area and pore volume using the Brunauer Emmett Teller (BET)

The MAC characteristics of salak seeds show that the surface area is 175.604 m^2/g, and the pore volume is 15.2334–38.2437 cc/g. Activated carbon made from snake fruit seeds has several advantages compared to that made from snake fruit skin, namely better surface morphology, pore

volume and specific surface area (Fathimah et al., 2021). MAC also has a larger surface area than activated carbon made from anthracite coal (Song et al., 2020), and from acrylic, coating materials, bentonite, distilled water, surfactants (epichlorohydrin-dimethylamine) (Azha and Ismail, 2021).

MAC morphology test with SEM-EDX equipment

The surface morphology and composition of ACSS elements are presented in Figure 6 and Table 2. Figure 6 shows that ACSS after carbonization process The surface is porous, rough, and has a complex structure. The cavities are visible and have many pores, with various sizes providing visual evidence of high porosity (Budianto et al., 2021; Kusdarini and Budianto, 2022). The test results using SEM-EDX also showed the damage of cellulose and hemicellulose in salak seeds that form this porous activated carbon structure (Ming-Ming Fu et al., 2019). ACSS after physical chemical activation has wider, more abundant pores, and a clearer pore structure than carbon after the carbonization process. Comparison of the element content of activated carbon after carbonization and after physical chemical activation is shown in Table 2.

Table 2. Composition of elements in activated carbon

Elemens	After carbonization (%)	After chemical physical activation (%)
C	83.8	90.5
O	13.2	9.3
Mg	0.1	0.1
P	0.4	-
S	0.2	-
Cl	0.6	-
K	1.6	0.1
Ca	0.1	-

Removal lead

Removal lead is calculated from the difference in Pb(II) content in the solution before contact and after contact with MAC. The percentage of lead removal in several concentrations of Pb(II) in solution after MAC contact are presented in Table 3. The percentage of Pb(II) removal was 96.81 – 97.97%, so the maximum adsorption capacity of MAC to Pb(II) in sample B is 35.49 mg/g.

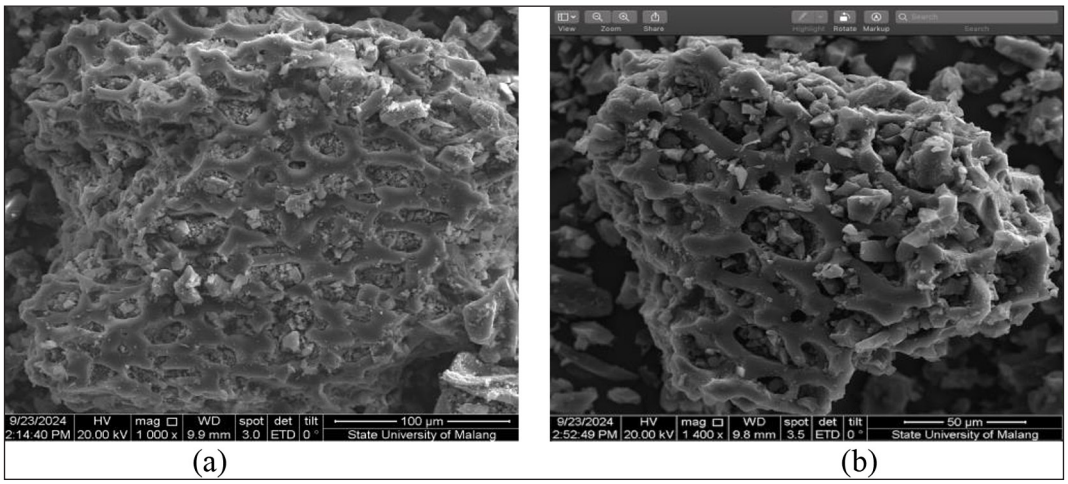

Figure 6. Appearance of the ACSS surface using SEM-EDX equipment: (a) after carbonization, (b) after chemical physical activation

Table 3. Lead removal percentage at various concentrations and samples

Sample	A	B	C	D	E
Co (mg/L)	36.44	30.37	24.29	18.22	12.15
Ce (mg/L)	0.95	0.97	0.5	0.37	0.28
Co- Ce (mg/L)	35.49	29.4	23.79	17.85	11.87
% removal Pb	97.39	96.81	97.94	97.97	97.70

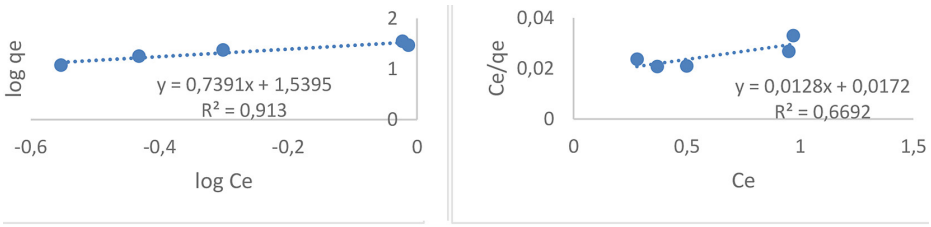

Figure 7. The plot of isotherm adsorption of Pb(II) by MAC from waste uses the following equations: (a) Freundlich Model, (b) Langmuir Model

Table 4. Isothermal parameters against Pb(II) adsorption by MAC

Adsorption system	Freundlich isotherm			Langmuir isotherm		
	R^2	*n*	K_F (mg/g)	R^2	*b* (L/mg)	q_m (mg/g)
Activated carbon	0.913	1.3530	34.634	0.6692	0.7442	78.125

Table 5. The concentration of Pb(II) ions on several contact time variables

T (min)	C_o (mg/L)	C_t (mg/L)	C_o-C_t (mg/L)	%A	C_o/C_t	$\ln(C_o/C_t)$	$1/C_t$ (L/mg)	q_e-q_t (mg/L)	log (q_e-q_t)	t/q_t
0	36.44	36.44	0	0	1	0	0.027442	35.56	1.550962	-
1	36.44	1.91	34.53	94.8	19.07853	2.948563	0.523560	1.03	0.012837	0.02896
3	36.44	1.79	34.65	95.1	20.35754	3.013451	0.558659	0.91	-0.04096	0.08658
5	36.44	1.67	34.77	95.4	21.82036	3.082843	0.598802	0.79	-0.10237	0.143802
10	36.44	1.73	34.71	95.3	21.06358	3.047546	0.578035	0.85	-0.07058	0.288101
30	36.44	0.89	35.55	97.6	40.94382	3.712201	1.123596	0.01	-2	0.843882
60	36.44	0.98	35.46	97.3	37.18367	3.615870	1.020408	0.1	-1	1.692047
75	36.44	0.9	35.54	97.5	40.48889	3.701028	1.1111111	0.02	-1.69897	2.110298

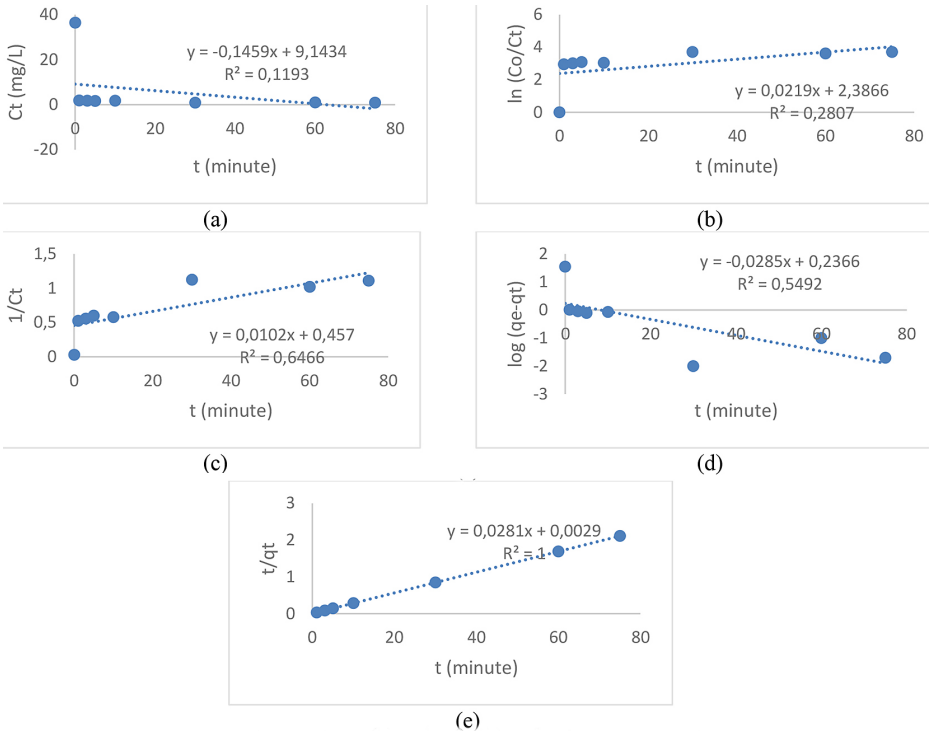

Figure 8. Ct vs t graph for reaction testing: (a) order 0, (b) order 1, (c) order 2, (d) pseudo order 1, (e) pseudo order 2

Adsorpsi isoterm

The ability of MAC to adsorb Pb(II) ions was also studied in an isotherm adsorption test using the MAC concentration variable in solution so that the ability of the adsorbent to absorb the adsorbate was known (Basu et al., 2018; Kusdarini et al., 2018, 2021). The test of activated carbon adsorption behavior on Pb(II) ions using the Freundlich and Langmuir equations is presented in Figure 7a and Figure 7b. Meanwhile, the isothermal parameters of Pb(II) ion adsorption by MAC are presented in Table 4.

Kinetics adsorption

Testing of the concentration of Pb(II) ions in $Pb(NO_3)_2$ solution that has been exposed to MAC for 1 – 75 minutes is presented in Table 5. Meanwhile, the reaction order testing of adsorption kinetic equations is presented in Figures 8a, 8b, 8c, 8d, and 8e.

The kinetics test of the Pb(II) adsorption reaction by MAC showed that R^2 was highest in the pseudo order 2 reaction. The constants resulting from 2nd order testing are q_e = 35.5872 mg/g, k_2 = 0.2723 g/mg.min and R^2 = 1.

CONCLUSIONS

The best operating conditions for MAC manufacturing are at a chemical activator concentration of H_3PO_4-HCl 2.05 M and a physical activation temperature of 600 °C. Activated carbon that has been activated by physical chemistry has a moisture content of 1–5%. Volatile matter 18.44–23.44%. Ash content 1–3%. Fixed carbon 68.56–78.56%. Iodine number 1205.7–1243.66 mg/g so that it meets the requirements of SNI 06-3730-1995. The SEM EDX test of activated carbon showed that the surface morphology of activated carbon that had been chemically activated by physics had wider pores and a clearer pore structure than the chemically activated carbon. The BET test produced findings that the surface area of activated carbon is 539.147 m^2/g and the pore radius is 44.0262–112.5906 cc/g so it has a very good potential to adsorb heavy metals. Activated carbon that has been activated by physical chemistry contains element C 90.5%. At 9.3%. And the rest of the elements Mg. K. Furthermore, MAC has the characteristics of 1% moisture content. 21.88% ash content. Volatile matter 38%. Fixed carbon 39.12%. And iodine number 1243.62 mg/g. MAC ash content has increased compared to the activated carbon ash content activated by physical chemistry due to the addition of Fe_3O_4 magnetic solution to activated carbon. Furthermore, the MAC adsorption ability test removes Pb(II) ions in wastewater by 94.8–97.6%. The adsorption of MAC isotherm to Pb(II) ions using the Freunlich equation yields the constants n = 1.3530, K_F = 34.634 mg/g, and R^2 = 0.91, while using the Langmuir equation produces the constants b = 0.7442 L/mg, q_m = 78.125 mg/g, and R^2 = 0.6692 so that it is more representative using the Freundlich equation than the Langmuir equation. Furthermore, for the testing of the MAC adsorption kinetics model on Pb(II) ions, it produced the best adsorption kinetic equation in the pseudo 2nd order reaction with R^2 = 1 and k_2 = 0.2737 g/mg.min.

Acknowledgments

Thank you to the Directorate of Research. Technology. And Community Service. Directorate General of Higher Education. Research. And Technology of the Ministry of Education. Culture. Research. And the Republic of Indonesia Technology for the financing that has been provided for Fundamental – Regular Research activities through the 2024 Research Grant contract number 109/E5/PG.02.00.PL/2024. 083/SP2H/PT/LL7/2024. and 02/KP/LPPM/ITATS/2024 so that the activity runs well and smoothly.

REFERENCES

1. Ahmad, F., & Manefield, M. (2024). Photosystem modulation and extracellular silicification in green microalgae: Key strategies for lead tolerance and removal. *Heliyon, 10*(16). https://doi.org/https://doi.org/10.1016/j.heliyon.2024.e36366
2. Ahmed, R. S., Abuarab, M. E., Baiomy, M. A., & Ibrahim, M. M. (2024). Heavy metals removal from industrial wastewater using bio-adsorbent materials based on agricultural solid wastes through batch and continuous flow mechanisms. *Journal of Water Process Engineering, 57*. https://doi.org/https://doi.org/10.1016/j.jwpe.2023.104665
3. Alam, S., Ilyas, M., Ullah, S., Zahoor, M., Naveed, M., & Ullah, R. (2024). Fabrication of magnetic activated carbon from corn-cob biomass for the removal of acidic dyes from wastewater. *Desalination and Water Treatment, 317*(December 2023),

100049. https://doi.org/10.1016/j.dwt.2024.100049

4. Ali, I., Burakov, A. E., Burakova, I. V., Kuznetsova, T. S., Ananyeva, O. A., Badin, D. A., … Imanova, G. (2024). Facile and economic preparation of graphene hydrothermal nanocomposite from sunflower waste: Kinetics, isotherms and thermodynamics for Cd(II) and Pb(II) removal from water. *Journal of Molecular Liquids, 407*. https://doi.org/https://doi.org/10.1016/j.molliq.2024.125179
5. Altintig, E., Onaran, M., Sarı, A., Altundag, H., & Tuzen, M. (2018). Preparation, characterization and evaluation of bio-based magnetic activated carbon for effective adsorption of malachite green from aqueous solution. *Materials Chemistry and Physics, 220*, 313–321. https://doi.org/10.1016/J.MATCHEMPHYS.2018.05.077
6. Azha, S. F., & Ismail, S. (2021). Feasible and economical treatment of real hand-drawn batik/textile effluent using zwitterionic adsorbent coating: Removal performance and industrial application approach. *Journal of Water Process Engineering, 41*, 1–12. https://doi.org/https://doi.org/10.1016/j.jwpe.2021.102093
7. Bagbi, Y., Yomgam, P., Libang, E., Boruah, B., Kaur, J., Jayanthi, S., … Dhania, N. K. (2024). Waste bamboo-derived magnetically separable bamboo-activated carbon: from characterization to effective remediation of fluoride (F−) ions from water††Electronic supplementary information (ESI) available. https://doi.org/10.1039/d4ra03752a. *RSC Advances, 14*(34), 24952–24968. https://doi.org/https://doi.org/10.1039/d4ra03752a
8. Basu, S., Ghosh, G., & Saha, S. (2018). Adsorption characteristics of phosphoric acid induced activation of bio-carbon: Equilibrium, kinetics, thermodynamics and batch adsorber design. *Process Safety and Environmental Protection, 117*, 125–142. https://doi.org/https://doi.org/10.1016/j.psep.2018.04.015
9. Beksissa, R., Tekola, B., Ayala, T., & Dame, B. (2021). Investigation of the adsorption performance of acid treated lignite coal for Cr (VI) removal from aqueous solution. *Environmental Challenges, 4*. https://doi.org/10.1016/J.ENVC.2021.100091
10. Budianto, A, Kusdarini, E., Mangkurat, W., Nurdiana, E., & Asri, N. (2021). Activated carbon producing from young coconut coir and shells to meet activated carbon needs in water purification process. *Journal of Physics: Conference Series. Surabaya: IOP Publishing*.
11. Budianto, Agus, Kusdarini, E., Amrullah, N. H., Ningsih, E., Udyani, K., & Aidawiyah. (2021). Physics and chemical activation to produce activated carbon from empty palm oil bunches waste *IOP Conference Series: Materials Science and Engineering, 1010*. https://doi.org/10.1088/1757-899X/1010/1/012016
12. Budianto, Agus, Pratiwi, A. G., Ningsih, S. A., & Kusdarini, E. (2023). Reduction of ammonia nitrogen and chemical oxygen demand of fertilizer industry liquid waste by coconut shell activated carbon in batch and continuous systems. *Journal of Ecological Engineering, 24*(7), 156–164. https://doi.org/https://doi.org/10.12911/22998993/164759
13. Cai, Y., Zheng, Z., Huang, Y., Xu, J., & Pan, J. (2025). Sequential super-assembled nanomotor adsorbents for NIR light-Powered blood lead removal. *Separation and Purification Technology*. https://doi.org/https://doi.org/10.1016/j.seppur.2024.129837
14. Chaurasia, A., & Kumar, A. (2024). Removal of mercury and lead ions from water using bioinspired N3Se3 type small sized moieties. *Chemical Communications, 60*(72), 9841–9844. https://doi.org/https://doi.org/10.1039/d4cc03587a
15. Fatimah, I., Sahroni, I., Dahlyani, M. S. E., Oktaviyani, A. M. N., & Nurillahi, R. (2021). Surfactant-modified Salacca zalacca skin as adsorbent for removal of methylene blue and Batik's wastewater. *Materials Today: Proceedings, 44*, 3211–3216. https://doi.org/https://doi.org/10.1016/j.matpr.2020.11.440
16. Gargiulo, V., Natale, F. Di, & Alfe, M. (2024). From agricultural wastes to advanced materials for environmental applications: Rice husk-derived adsorbents for heavy metals removal from wastewater. *Journal of Environmental Chemical Engineering, 12*(5). https://doi.org/https://doi.org/10.1016/j.jece.2024.113497
17. Gong, Y., Gai, L., Tang, J., Fu, J., Wang, Q., & Zeng, E. Y. (2017). Reduction of Cr(VI) in simulated groundwater by FeS-coated iron magnetic nanoparticles. *Science of The Total Environment, 595*, 743–751. https://doi.org/https://doi.org/10.1016/j.scitotenv.2017.03.282
18. Ismail, U. M., Ibrahim, A. I., Onaizi, S. A., & Vohra, M. S. (2024). Synthesis and application of MgCuAl-layered triple hydroxide/ carboxylated carbon nanotubes/bentonite nanocomposite for the effective removal of lead from contaminated water. *Results in Engineering*, 1–12. https://doi.org/https://doi.org/10.1016/j.rineng.2024.102991
19. Kusdarini, E., & Budianto, A. (2022). Characteristics and adsorption test of activated carbon from Indonesian bituminous coal. *Journal of Ecological Engineering, 23*(10), 1–15. https://doi.org/https://doi.org/10.12911/22998993/152343
20. Kusdarini, E., Pradana, D. R., & Budianto, A. (2022). Production of activated carbon from high-grade bituminous coal to removal Cr(VI). *Reaktor, 22*(1), 14–20. https://doi.org/https://doi.org/10.14710/reaktor.22.1.14-20
21. Kusdarini, E., Purwaningsih, D. Y., & Budianto, A. 2018. Adsorption of Pb2+ Ion in Water Well with Amberlite Ir 120 Na Resin. *Pollution Research,*

37(4), 307–312.

22. Kusdarini, E., Purwaningsih, D. Y., & Budianto, A. (2021). Removal Pb2+ of Well Water using Purolite C-100 Resin and Adsorption Kinetic. *Pollution Research, 40*(2).
23. Kusdarini, E., Sania, P. R., & Budianto, A. (2023). Adsorption of iron and manganese ions from mine acid water using manganese green sand in batch process. *Journal of Ecological Engineering, 24*(12), 158–166.
24. Liu, W., Jin, L., Xu, J., Liu, J., Li, Y., Zhou, P., … Wang, X. (2019). Insight into pH dependent Cr(VI) removal with magnetic Fe3S4. *Chemical Engineering Journal, 359*, 564–571. https://doi.org/https://doi.org/10.1016/j.cej.2018.11.192
25. Messaoudi, N. El, Miyah, Y., Şenol, Z. M., Ciğeroğlu, Z., Kazan-Kaya, mine S., Gubernat, S., … Franco, D. S. P. (2024). Comprehensive analytical review of heavy metal removal efficiency using agricultural solid waste-based bionanocomposites. *Nano-Structures & Nano-Objects, 38*. https://doi.org/https://doi.org/10.1016/j.nanoso.2024.101220
26. Ming-Ming Fu, Mo, C.-H., Li, H., Zhang, Y.-N., Huang, W.-X., & Wong, M. H. (2019). Comparison of physicochemical properties of biochars and hydrochars produced from food wastes. *Journal of Cleaner Production, 236*. https://doi.org/https://doi.org/10.1016/j.jclepro.2019.117637
27. Mohamed, W. R., Mohamed, T. M., Hamed, M. M., Metwally, S. S., & Borai, E. H. (2024). Evaluation of synthetic PVP-HEMA as a polymeric material for the removal of lead ions from aqueous solutions. *Journal of Radiation Research and Applied Sciences, 17(*4). https://doi.org/https://doi.org/10.1016/j.jrras.2024.101145
28. Nowruzi, R., Heydari, M., & Javanbakht, V. (2020). Synthesis of a chitosan/polyvinyl alcohol/activate carbon biocomposite for removal of hexavalent chromium from aqueous solution. *International Journal of Biological Macromolecules, 147*, 209–216.
29. Pochampally, S. V., Letourneau, E., Abdulraheem, I., Monk, J., Sims, D., Murph, S. E. H., … Moon, J. (2024). Metal-organic-framework and walnut shell biochar composites for lead and hexavalent chromium removal from aqueous environments. *Chemosphere.* https://doi.org/https://doi.org/10.1016/j.chemosphere.2024.143572
30. Polii, F. F. (2017). Pengaruh suhu dan lama aktifasi terhadap mutu arang aktif dari kayu kelapa. (Effects of Activation Temperature and Duration Time on the Quality of the Active Charcoal of Coconut Wood). *Jurnal Industri Hasil Perkebunan, 12*(2), 21–28. https://doi.org/10.33104/jihp.v12i2.1672
31. Samanth, A., Selvaraj, R., & Murugesan, G. (2024). Chemosphere using biomass derived magnetic activated carbon nanocomposite in synthetic and simulated agricultural runoff water. 361(February).
32. Song, G., Deng, R., Yao, Z., Chen, H., Romero, C., Lowe, T., … Baltrusaitis, J. (2020). Anthracite coal-based activated carbon for elemental Hg adsorption in T simulated flue gas: *Preparation and evaluation. Fuel, 275*, 1–10. https://doi.org/https://doi.org/10.1016/j.fuel.2020.117921
33. Ton-That, L., Nguyen, T.-P.-T., Duong, B.-N., Nguyen, D.-K., Nguyen, N.-A., Ho, T., & Dinh, V.-P. (2024). Insights into Pb (II) adsorption mechanisms using jackfruit peel biochar activated by a hydrothermal method toward heavy metal removal from wastewater. *Biochemical Engineering Journal, 212*. https://doi.org/https://doi.org/10.1016/j.bej.2024.109525
34. Vaddi, D. R., & Malla, R. (2024). Magnetic activated carbon_ A promising approach for the removal of methylene blue from wastewater. *Desalination and Water Treatment, 317*(February), 100146. https://doi.org/10.1016/j.dwt.2024.100146
35. Wei, B., Ji, Z., Xu, Y., Kong, S., Zhang, Y., & Li, C. (2023). Magnetic modified chitosan composites for hexavalent chromium removal. 311, 155–161. https://doi.org/10.5004/dwt.2023.30001
36. Yagub, M. T., Sen, T. K., Afroze, S., & Ang, H. M. (2014). Dye and its removal from aqueous solution by adsorption: A review. *Advances in Colloid and Interface Science, 209*, 172–184. Elsevier. https://doi.org/10.1016/j.cis.2014.04.002
37. Yang, F., Jin, C., Wang, S., Wang, Y., Wei, L., Zheng, L., … Sonne, C. (2023). Chemosphere Bamboo-based magnetic activated carbon for efficient removal of sulfadiazine : Application and adsorption mechanism. *Chemosphere, 323*(January), 138245. https://doi.org/10.1016/j.chemosphere.2023.138245
38. Yokwana, K., Nagare, H., Ntsendwana, B., Ogunlaja, A. S., & Mhlanga, S. D. (2024). Flagella, palmella and cyst *Haematococcus lacustris* microalgae cells decorated on graphene oxide and graphene nanoplatelets-activated carbon as novel adsorbents for the removal of lead from water. *Physics and Chemistry of the Earth, Parts A/B/C*. https://doi.org/https://doi.org/10.1016/j.pce.2024.103778
39. Yue, Z., Economy, J., & Mangun, C. L. (2003). Preparation of fibrous porous materials by chemical activation 2. *H3PO4 activation of polymer coated fibers. Carbon, 41*(9), 1809–1817. https://doi.org/10.1016/S0008-6223(03)00151-9